

Grain Size Analysis of Karli River Estuarine Sediments Sindhudurg, Maharashtra, India.

Shivani hulaji¹, Nagaraju.D¹, Balasubramanian.A¹, Siddaraju.K¹ and Honamgond.P.T²

¹Department of Studies in Earth Science, University of Mysore, Mysore-570006, Karnataka.

²Associate Professor and Head of Department of Geology, GSSc College, Belagavi, Karnataka.
Email-mayanaga_raju@yahoo.co.in, siddesh.12@gmail.com, emmrc1@gmail.com

ABSTRACT

Estuaries are coastal ecological niche, receiving importance in recent years due to industrialization, urbanization, and construction of harbors along their bank. The estuaries have also gained importance and attracted the attention of scientists, administrators and ecologists in view of their biodiversity. Most of the estuarine areas are put into various uses, such as constant source of fish supply for coastal population, with high agriculture potential used for cultivation, habitat for birds, recreation, navigation, bird watching, domestic use, disposal of industrial waste and sewage. Estuaries are ideal grounds for aquaculture. The estuarine environment is recognized as a complex ecosystem with widely varying physico-chemical influences and characteristic biota. Sediment composition within the estuaries is a major controlling factor which depends on the type and amount of material released from the catchment area of a river. The rivers within tropical climatic zones are bound to release higher quantity of transported material into the estuaries due to the humid climate. Once released into the aquatic environment, trace metals may also interact with suspended matter, and subsequently be removed from the water column facilitating deposition. Metal concentration in sediments within estuaries can be influenced by several factors such as salinity, freshwater discharge, flow rates and geomorphological conditions. Further, sediments composed of different geochemical phases such as clay, silt, sand, organic material, oxides of iron and manganese, carbonates and sulphide complexes, act as potential binding sites for metals entering an estuarine system. Metals are natural constituents, but anthropogenic activities can cause elevated levels of these metals in various parts of the system. Once the metal concentration exceeds certain level, they may lead to severe environmental problems.

Key words: Industrial wastes, Organic material, Estuaries, aquatic environment and anthropogenic activities.

Date of Submission: 04-10-2017

Date of acceptance: 18-10-2017

I. INTRODUCTION:

Knowledge of the textural characteristics of the estuarine sediments is of great importance in differentiating various depositional environments. By virtue of their characteristics and location, estuaries have been of great interest to coastal geomorphologists and physical oceanographers. It is also known since long time that the coastal and estuarine waters are among the most productive ecosystems on Earth, providing numerous ecological, economic, cultural, recreational and aesthetic benefits and services to mankind. However, they are also among the most threatened eco-systems by flooding and erosion, largely as a result of the extreme hydrological conditions such as storm waves during cyclones, high tides and floods. The estuaries on the western Indian coast are quite numerous as compared to the east coast of India. This is mainly due to the presence of Western Ghats, providing numerous river and

backwater systems that contributed formation of numerous estuaries along the west coast. An estuary is a semi-enclosed coastal body of water which has a free connection with the open sea and within which sea water is measurably diluted with fresh water derived from land drainage.

II. STUDY AREA

The Karli River of southern Maharashtra originates from the Western Ghats of India. Its Geographical location is between 16° 0'17.50"N 73°29'46.60"E and 16° 4'48.31"N 74° 0'15.35"E, which flows through Sindhudurg district and meets the Arabian sea near Devbag beach and Bhogwa beach (Fig 1).

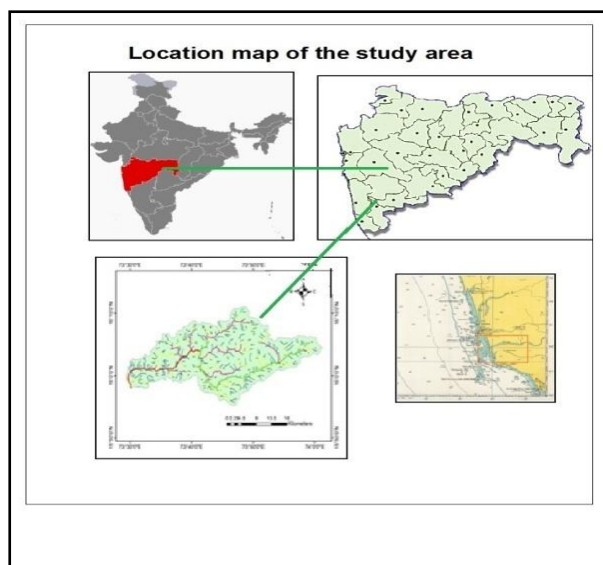


Fig.1 Location Map of the study area

III. METHODS AND MATERIALS

To study the grain size variation and depositional environment, the estuarine portion of Karli river has been sampled on the 11 November 2016. Overall, 25 sediment samples were collected at every 500m distance and are used in the present study.

3.1 Data Sets used

The data used in the work is comprised of field data on estuarine water (surface and bottom) and sediment from the Karli river (estuarine part). The change detection, estuarine landforms etc were studied using remote sensing data. The data used and their sources are given below (Table 1).

DATA USED	SOURCE
Base map	Survey of India, Toposheet, (47 H/8) on 1:2,00,000 scale.
Satellite Data	LANDSAT TM.
Digital Elevation Model	SRTM (Shuttle Radar Topography Mission) data
INFRASTRUCTURE FACILITIES	
GPS (Garmin)	
Application of Remote Sensing	ERDAS IMAGINE 9.3 software procured through MOES Project Grants.
Sand-silt-clay analysis, Sieve analysis	Laboratory
XRD Analysis	Laboratory
Beach profile and sedimentological Data.	Field

Table.1 Data Used

IV. RESULTS AND DISCUSSION

4.1 Geology of the area

The Sindhudurg district exhibits wide range of geological formations (recent sediments, residual lateritic, basaltic flows, schists, granites, gabbro, quartzites etc, with variety of dykes). A greater part of the coastal belt of Maharashtra is developed as a result of several morpho-dynamic cycles. The basement of basalt flows was formed by extruded Deccan Volcanic activity during Late Cretaceous – Early Tertiary period with a minor metamorphosed Dharwar in the southernmost section of Sindhudurg. The Precambrian granites and gneisses, quartzites and amphibolites are exposed in the region around Vengurla that continues up to the Karwar (Karnataka state). The coast displays a variety of landforms developed due to fluvial and marine activity, both erosional and depositional during the Tertiary and Quaternary periods (Fig.2).

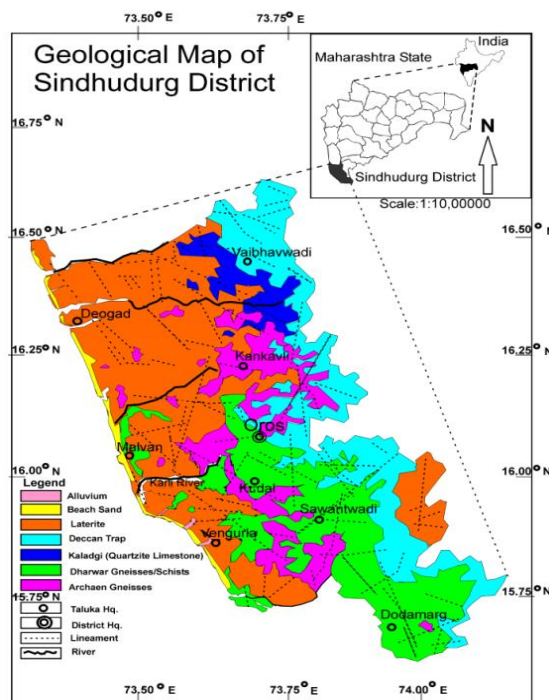


Fig.2 Geological Map of the area

4.2 Granulometry:

To understand the sediment dynamics and environment of deposition, it is necessary to know first, the particle size distribution. The type of analysis depends upon the nature of sediment available in the environment. The representative samples were washed to remove salts and tests of micro organisms like foraminifers. The bigger shell fragments were hand-picked and later the samples were dried in natural conditions. Representative proportions were obtained by coning and

quartering and were treated chemically to remove carbonate material, Iron coating and organic contents (Table 2).

Table 2 Chemicals used for various purposes:

Sl. No	CHEMICALS USED	PURPOSE
1	Dil Hydrochloric acid – 1N	To dissolve Calcium Carbonates
2	Oxalic Acid and Al coin	To remove Iron content
3	Hydrogen peroxide	To remove organic content

The treated samples were dried, weighed and then subjected to sieve analysis. The samples were analyzed at quarter phi intervals on a Ro-Tap sieve shaker using ASTM (American Society for Testing and Materials) sieves for 15 min. The sieve data (weight percent - cumulative weight percentages) was used to calculate grain size parameters using Gradisat computer program (Blott and Pye, 2001) both for graphic (Folk and Ward's, 1957) and moment (Friedman, 1967) method. The weight percent data was used for EOF analysis.

4.3 Sediment Transport Model (STM):

The method of McLaren and Bowels (1884) is utilized to understand the transport trends in the wave dominated environment, using grain size parameters computed following Friedman's (1967). The analytical method is known as sediment trend analysis. The purpose is to provide a rapid undertaking of the direction of sediment transport moment and to define the areas of erosion, accretion and equilibrium. McLaren (1981) suggested that the mean size, sorting and skewness of grain size frequency distribution follow trends that identify the direction of transport and the sedimentary processes of winnowing, selective deposition and total deposition. Using hypothetical sediment distribution an assumption "light grains have a greater probability of being eroded and transported than heavy grains". He demonstrated that:

- Sediment in transport must be finer, better sorted and more negatively skewed than its source sediment.
- A lag must become coarser, better sorted and more positively skewed.
- Successive deposits may become finer and coarser, but the sorting must become better and the skewness more positive.

4.4 X-Ray Diffraction analysis (XRDA):

X-ray powder diffraction (XRD) is a rapid analytical technique primarily used for phase

identification of a crystalline material and can provide information on unit cell dimensions. The analyzed material is finely ground, homogenized and average bulk composition is determined. In XRD analysis, a focused X-Ray beam is shot at the sample at a specific angle of incidence. The X-Rays deflect or "diffract" in various ways depending on the crystal structure (inter-atomic distances) of the sample. The locations (angles) and intensities of the diffracted X-Rays are measured.

4.5 Fundamental Principles of X-ray Powder Diffraction (XRD):

X-ray diffraction is based on constructive interference of monochromatic X-rays and a crystalline sample. These X-rays are generated by a cathode ray tube, filtered to produce monochromatic radiation, collimated to concentrate, and directed toward the sample. The organic matter in the sample was removed using H₂O₂. The sample was then wet-sieved through a 230 (0.063 mm) ASTM sieve and homogeneous suspension was obtained after repeated washing and decanting and sample was subjected to XRD analysis. The data obtained from this process is given in the Table 3 and Figures A to D below. For the interpretation of this data obtained, a software called Match 3.4 version has been used. As per the data obtained by analyzing the samples taken at the samples 5, 17 and 22, we can find variations in the mineralogy i.e. as per the match phase report, sample 5 consists of illite in abundance, and sample 17 has quartz and also contains sufficient quantity of illite. But illite may be absent (or if present its only in trace quantity), quartz is sufficiently present with the abundancy of H₂ N₄ Ni S₄. The presence of the products of lanthanum manganese copper phosphide and Titanomagnetite are also found to be present along with some amount of trillithium gallium trimolybdate.

**Table 3 XRDA Results
 Sample: 5 Matched Phases**

Index	Amount (%)	Name	Formula sum
A	52.4	Illite	Al ₄ KO ₁₂ Si ₂
B	32.9	Quartz	SiO ₂
C	11.1	trillithium gallium trimolybdate	Ga Li ₃ Mo ₃ O ₁₂
D	3.6	lanthanum manganese copper phosphide	Cu ₉ La ₂ Mn ₃ P ₇
	22.1	Unidentified peak area	

Sample 17: Matched Phases

Index	Amount (%)	Name	Formula sum
A	55.1	Quartz	SiO ₂
B	37.5	Illite	Al ₄ H ₂ KO ₁₂ Si ₄
C	7.3	Magnetite	Fe ₃ O ₄
	71.7	Unidentified peak area	

Sample 22: Matched Phases

Index	Amount (%)	Name	Formula sum
A	58.0	Ni(HN ₂ S ₂) ₂	H ₂ N ₄ NiS ₄
B	33.7	Quartz	SiO ₂
C	8.2	Titanomagnetite	Fe _{2.5} O ₄ Ti _{0.5}
	71.3	Unidentified peak area	

Sample: 5 Matched Phases

No.	2theta [°]	d [Å]	I/I0	FWHM	Matched
1	19.84	4.4716	49.23	0.52	A,C
2	19.99	4.4383	63.03	0.52	A,C
3	20.6	4.3078	103.06	0.52	A,C
4	20.89	4.248	176.79	0.52	A,B
5	22.01	4.0345	65.7	0.52	C
6	22.57	3.9355	68.36	0.52	A,D
7	22.98	3.8666	46.3	0.52	A
8	23.54	3.7756	128.72	0.52	C
9	23.84	3.7297	35.48	0.52	A
10	24.83	3.5828	43.94	0.52	A,C
11	25.4	3.5037	45.53	0.52	A,D
12	26.13	3.4074	125.78	0.52	C
13	26.57	3.3526	100	0.52	A,B,C
14	26.81	3.3226	415	0.52	C
15	27.67	3.2208	83.55	0.52	A
16	28.47	3.133	41.65	0.52	A,C,D
17	29.27	3.0486	53.06	0.52	C
18	29.51	3.0243	118.36	0.52	D
19	29.71	3.0044	46.66	0.52	A
20	29.98	2.9777	105.81	0.52	C
21	30.64	2.9151	43.3	0.52	C
22	31.79	2.8125	48.1	0.52	A,C
23	32.48	2.7542	138.57	0.52	C
32	32.84	2.7253	97.7	0.52	
24	34.45	2.6009	68.85	0.52	A,C
25	34.73	2.5812	123.61	0.52	A
26	35.18	2.549	116.03	0.52	A,C
27	35.48	2.5278	149.63	0.52	C
28	35.83	2.5041	67.78	0.52	A,C
29	36.24	2.477	65.24	0.52	A
30	36.64	2.4507	473.63	0.52	A,B,C,D
31	37.81	2.3772	108.92	0.52	A
32	38.3	2.3482	46.6	0.52	A
33	38.84	2.317	48.43	0.52	A,C,D
34	39.24	2.2938	89.36	0.52	B,C
35	39.89	2.2583	43.79	0.52	A,C,D
36	40.31	2.2356	75.76	0.52	A,B,C
37	40.9	2.2045	43.12	0.52	A,C
38	41.12	2.1936	41.96	0.52	A,C

39	41.51	2.1738	41.49	0.52	C
40	41.9	2.1545	60.38	0.52	A,C
41	42.29	2.1353	121.85	0.52	A,B,C
42	43.39	2.0836	46.11	0.52	A,D
43	43.75	2.0672	39.99	0.52	A,C
44	44.21	2.0472	165.68	0.52	A,C,D
45	45.06	2.0104	63.84	0.52	A,C
46	45.57	1.989	52.71	0.52	A,C,D
47	45.84	1.9781	73.15	0.52	A,B,C
48	47.34	1.9187	41.91	0.52	C,D
49	47.84	1.8999	40.8	0.52	A,C,D
50	48.68	1.869	164.43	0.52	A,C
51	49.2	1.8505	60.19	0.52	A,C
52	49.73	1.8321	152.17	0.52	C,D
53	50.09	1.8197	215.37	0.52	B,D
54	50.29	1.8128	36.26	0.52	C,D
55	50.75	1.7976	54.49	0.52	B,C
56	51.32	1.779	52.11	0.52	A,C
57	52.68	1.7362	44.74	0.52	A,C
58	52.88	1.7301	36.69	0.52	C
59	53.24	1.7192	50.79	0.52	A,D
60	53.78	1.7033	79.39	0.52	A,C
61	54.01	1.6963	37.6	0.52	A,C
62	54.7	1.6766	96.6	0.52	A,C
63	54.84	1.6727	77.28	0.52	A,B,C,D
64	55.7	1.649	44.01	0.52	A,C,D
65	56.23	1.6345	85.64	0.52	A
66	56.38	1.6306	56.76	0.52	A,C
67	56.69	1.6226	62.98	0.52	A
68	57.32	1.606	58.5	0.52	A,B,C,D
69	58.87	1.5676	99.17	0.52	A,C
70	59.11	1.5616	43.52	0.52	A

Sample 17: Matched Phases

No.	2theta [°]	d [Å]	I/I0	FWHM	Matched
1	18.38	4.8221	28.39	0.2	C
4	18.78	4.7211	27.56	0.2	
2	19.55	4.5374	31.9	0.2	B
3	20.43	4.3435	26.59	0.2	B
4	20.9	4.2466	119.57	0.2	A
5	21.68	4.0955	42.72	0.2	B
6	23.13	3.8418	184.91	0.2	B
7	24.26	3.6655	42.9	0.2	B
8	26.84	3.3191	100	0.2	A,B
9	28.83	3.0942	120.43	0.2	B
10	30.13	2.9637	93.91	0.2	C
11	30.62	2.9173	76.23	0.2	B
12	33.6	2.6649	28.01	0.2	B
13	34.25	2.6158	27.01	0.2	B
14	34.68	2.5849	33.13	0.2	B
15	34.87	2.5706	58.35	0.2	B
16	35.17	2.5497	71.08	0.2	B
17	35.57	2.5221	153	0.2	C
18	36	2.4927	132.01	0.2	B
19	36.3	2.473	141.63	0.2	B

20	36.47	2.4617	37.35	0.2	B
21	36.67	2.4487	36.08	0.2	A,B
22	37.12	2.4203	51.57	0.2	C
23	39.77	2.2649	63.43	0.2	A,B
24	40.4	2.2306	28.02	0.2	A
25	40.7	2.2149	56.98	0.2	B
26	41.01	2.1991	28.47	0.2	B
27	42.63	2.1193	95.42	0.2	A
28	42.91	2.1059	79.4	0.2	B
29	43.31	2.0877	28.91	0.2	B,C
30	44.77	2.0225	43.26	0.2	B
31	45.81	1.9791	81.1	0.2	B
32	45.93	1.9743	36.15	0.2	A
33	46.68	1.9444	30.08	0.2	B
34	47.28	1.9211	35.35	0.2	C
35	47.54	1.9112	26.88	0.2	B
36	48.2	1.8865	30.25	0.2	B
37	48.78	1.8653	30	0.2	B
38	50.03	1.8216	35.35	0.2	B
39	50.39	1.8094	156.75	0.2	A
40	50.94	1.7911	66.29	0.2	A
41	52.17	1.7519	26.52	0.2	B
42	53.56	1.7096	26.04	0.2	B,C
43	53.8	1.7025	50.74	0.2	B
44	54.1	1.6938	31.62	0.2	B
45	54.4	1.6852	41.95	0.2	B
46	54.66	1.6779	36.29	0.2	B
47	55.11	1.6652	90.16	0.2	A,B
48	55.27	1.6607	47.17	0.2	B
49	55.51	1.6541	63.5	0.2	A,B
50	55.88	1.644	37.22	0.2	B
51	56.35	1.6315	39.25	0.2	B
52	57.13	1.6109	53.33	0.2	C
53	57.58	1.5995	30.61	0.2	A,B
54	57.84	1.5929	28.99	0.2	B
55	58.35	1.5801	29.8	0.2	B

Sample 22: Matched Phases

No.	2theta [°]	d [Å]	I/I0	FWHM	Matched
1	14.01	6.317	26.5	0.16	A
2	14.23	6.2194	30.64	0.16	A
3	15.55	5.6953	30.77	0.16	A
4	18.08	4.9036	56.28	0.16	C
5	18.24	4.8595	62.61	0.16	A
6	18.75	4.7295	50.67	0.16	A
7	19.02	4.6624	71.89	0.16	A
8	20.94	4.2399	180.9	0.16	A,B
9	21.95	4.0453	69.54	0.16	A
10	22.22	3.9976	59.79	0.16	A
11	22.49	3.9502	54.22	0.16	A
12	23.24	3.825	67.22	0.16	A
13	23.54	3.7758	160.86	0.16	A
14	23.69	3.7527	110.97	0.16	A
15	24.35	3.652	86.83	0.16	A
16	24.73	3.5965	48	0.16	A
17	25.38	3.5071	51.86	0.16	A

18	25.56	3.4827	92.29	0.16	A
19	25.9	3.4373	37.45	0.16	A
20	26.16	3.4037	59.48	0.16	A
21	26.47	3.364	1000	0.16	A,B
22	26.81	3.3221	72.6	0.16	A
23	27.18	3.2779	58.54	0.16	A
24	27.43	3.249	92.81	0.16	A
25	28.25	3.156	77.15	0.16	A
26	28.68	3.1096	37.7	0.16	A
27	28.82	3.0952	34.61	0.16	A
28	29.1	3.0658	37.29	0.16	A
29	29.48	3.0275	66.6	0.16	A
30	29.8	2.9958	111.3	0.16	C
31	29.94	2.982	60.67	0.16	A
32	30.05	2.9714	41.31	0.16	A
33	30.24	2.9532	93.48	0.16	A
34	30.69	2.9109	50.97	0.16	A
35	30.96	2.8862	33.14	0.16	A
36	31.31	2.855	104.75	0.16	A
37	31.46	2.8413	46.16	0.16	A
38	33.6	2.6653	82.72	0.16	A
39	34.43	2.6028	30.53	0.16	A
40	34.85	2.5723	53.26	0.16	A
41	34.98	2.5631	29.4	0.16	A
42	35.25	2.5438	126.62	0.16	A,C
43	35.42	2.5322	106.98	0.16	A
44	35.69	2.5136	44.22	0.16	A
45	36.16	2.482	27.37	0.16	A
46	36.46	2.4626	45.99	0.16	A,B
47	36.65	2.45	43.79	0.16	A
48	36.76	2.4429	24.71	0.16	C
49	36.96	2.43	52.83	0.16	A
50	37.93	2.3705	25.09	0.16	A
51	38.24	2.3516	30.97	0.16	A
52	39.04	2.3054	55.7	0.16	A
53	39.38	2.2862	50.98	0.16	A,B
54	40.06	2.2488	51.15	0.16	A
55	40.37	2.2324	43.02	0.16	A,B
56	40.5	2.2255	33.98	0.16	A
57	41.74	2.1623	60.83	0.16	A
58	42.14	2.1428	69.39	0.16	A
59	42.37	2.1315	57.81	0.16	A,B
60	42.52	2.1244	36.92	0.16	A
61	42.78	2.1122	23.89	0.16	A,C
62	43.55	2.0764	42.93	0.16	A
63	44.24	2.0458	32.39	0.16	A
64	44.52	2.0334	34.64	0.16	A
65	44.72	2.0248	25.2	0.16	A
66	45.18	2.0054	36.66	0.16	A
67	45.43	1.995	36.38	0.16	A
68	45.54	1.9904	34.64	0.16	A
69	45.75	1.9816	39.34	0.16	A,B
70	46.09	1.9677	36.88	0.16	A
71	46.6	1.9475	43.47	0.16	A
72	46.78	1.9404	38.7	0.16	C
73	46.96	1.9333	21	0.16	A

74	47.37	1.9174	39	0.16	A
75	47.55	1.9106	29.48	0.16	A
76	47.75	1.9033	24.23	0.16	A
77	48.08	1.891	39.35	0.16	A
78	48.25	1.8845	38.06	0.16	A
79	48.46	1.8769	30.47	0.16	A
80	48.75	1.8665	49.96	0.16	A
81	48.98	1.8582	23.34	0.16	A
82	49.3	1.8469	22.86	0.16	A
83	49.57	1.8373	46.84	0.16	A
84	49.84	1.8281	52.49	0.16	A
85	49.98	1.8234	51.04	0.16	A,B
86	50.21	1.8157	27.86	0.16	A
87	50.67	1.8002	29.13	0.16	A,B
88	50.78	1.7965	25.83	0.16	A
89	51.38	1.777	36.17	0.16	A
90	51.75	1.7652	21.48	0.16	A
91	51.97	1.7581	26.86	0.16	A
92	52.24	1.7497	21.73	0.16	A
93	52.98	1.7269	78.59	0.16	A,C
94	53.23	1.7194	44.47	0.16	A
95	53.95	1.6983	30.07	0.16	A
96	54.11	1.6936	27.36	0.16	A
97	54.34	1.6868	23.2	0.16	A
98	54.66	1.6777	29.53	0.16	A
99	54.82	1.6732	58.74	0.16	A,B
100	55.3	1.6599	20.78	0.16	A,B
101	55.64	1.6505	30.68	0.16	A
102	56.07	1.6389	34.1	0.16	A
103	56.43	1.6293	37.65	0.16	A,C
104	56.58	1.6253	24.4	0.16	A
105	56.92	1.6165	38.53	0.16	A
106	57.09	1.612	24.62	0.16	A,B
107	57.38	1.6046	54.36	0.16	A
108	57.62	1.5984	21.27	0.16	A
109	57.84	1.5929	36.92	0.16	A
110	58.16	1.5849	38.17	0.16	A
111	58.36	1.5798	26.67	0.16	A
112	58.5	1.5764	24.87	0.16	A
113	58.65	1.5728	21.86	0.16	A
114	58.84	1.5681	23.72	0.16	A
115	59.03	1.5636	27.81	0.16	A
116	59.41	1.5545	23.61	0.16	A
117	59.81	1.545	39.35	0.16	A,B

4.5 Textural Analysis (TA):

A grain size distribution analysis statistical package was used evaluate the Unconsolidated Sediments by Sieving or Laser Granulometer. The program is best suited to analyse data obtained from sieve or laser granulometer analysis. The user is required to input the mass or percentage of sediment retained on sieves spaced at any intervals, or the percentage of sediment detected in each bin of a Laser Granulometer. The following sample statistics are then calculated using the Method of Moments in

Microsoft Visual Basic programming language: mean, mode(s), sorting (standard deviation), skewness, kurtosis. Grain size parameters are calculated arithmetically and geometrically (in microns) and logarithmically (using the phi scale) (Krumbein and Pettijohn, 1938. Linear interpolation is also used to calculate statistical parameters by the Folk and Ward (1957) graphical method and derive physical descriptions (such as “very coarse sand” and “moderately sorted”). The program also provides a physical description of the textural group which the

sample belongs to and the sediment name (such as “fine gravelly coarse sand”) after Folk (1954). Also included is a table giving the percentage of grains falling into each size fraction, modified from Udden (1914) and Wentworth (1922). In terms of graphical output, the program provides graphs of the grain size

distribution and cumulative distribution of the data in both metric and phi units, and displays the sample grain size on triangular diagrams. Samples may be analysed singularly, or up to 250 samples may be analysed together (Table 3 and 4).

Table 3.1 Statistical formulae used in the calculation of grain size parameters.

f is the frequency in percent; m is the mid-point of each class interval in metric (m_m) or phi (m_ϕ) units; P_x and ϕ_x are grain diameters, in metric or phi units respectively, at the cumulative percentile value of x .

(a) Arithmetic Method of Moments

Mean	Standard Deviation	Skewness	Kurtosis
$\bar{x}_a = \frac{\sum f m_m}{100}$	$\sigma_a = \sqrt{\frac{\sum f (m_m - \bar{x}_a)^2}{100}}$	$Sk_a = \frac{\sum f (m_m - \bar{x}_a)^3}{100\sigma_a^3}$	$K_a = \frac{\sum f (m_m - \bar{x}_a)^4}{100\sigma_a^4}$

(b) Geometric Method of Moments

Mean	Standard Deviation	Skewness	Kurtosis
$\bar{x}_g = \exp \frac{\sum f \ln m_m}{100}$	$\sigma_g = \exp \sqrt{\frac{\sum f (\ln m_m - \ln \bar{x}_g)^2}{100}}$	$Sk_g = \frac{\sum f (\ln m_m - \ln \bar{x}_g)^3}{100 \ln \sigma_g^3}$	$K_g = \frac{\sum f (\ln m_m - \ln \bar{x}_g)^4}{100 \ln \sigma_g^4}$

Sorting (σ_g)	Skewness (Sk_g)	Kurtosis (K_g)
Very well sorted	< 1.27	Very fine skewed < 1.30
Well sorted	1.27 – 1.41	Fine skewed 1.30 – 0.43
Moderately well sorted	1.41 – 1.62	Symmetrical 0.43 – +0.43
Moderately sorted	1.62 – 2.00	Coarse skewed +0.43 – +1.30
Poorly sorted	2.00 – 4.00	Very coarse skewed > +1.30
Very poorly sorted	4.00 – 16.00	
Extremely poorly sorted	> 16.00	

(c) Logarithmic Method of Moments

Mean	Standard Deviation	Skewness	Kurtosis
$\bar{x}_\phi = \frac{\sum f m_\phi}{100}$	$\sigma_\phi = \sqrt{\frac{\sum f (m_\phi - \bar{x}_\phi)^2}{100}}$	$Sk_\phi = \frac{\sum f (m_\phi - \bar{x}_\phi)^3}{100\sigma_\phi^3}$	$K_\phi = \frac{\sum f (m_\phi - \bar{x}_\phi)^4}{100\sigma_\phi^4}$

Sorting (σ_ϕ)	Skewness (Sk_ϕ)	Kurtosis (K_ϕ)
Very well sorted	< 0.35	Very fine skewed > +1.30
Well sorted	0.35 – 0.50	Fine skewed +0.43 – +1.30
Moderately well sorted	0.50 – 0.70	Symmetrical 0.43 – +0.43
Moderately sorted	0.70 – 1.00	Coarse skewed 0.43 – 1.30
Poorly sorted	1.00 – 2.00	Very coarse skewed < 1.30
Very poorly sorted	2.00 – 4.00	
Extremely poorly sorted	> 4.00	

Table 3.2 Size scale adopted in the GRADISTAT program, modified from Udden (1914) and Wentworth (1922).

Grain Size		Descriptive term	
phi	mm		
-10	1024	Very Large	} Boulder
-9	512	Large	
-8	256	Medium	
-7	128	Small	
-6	64	Very small	
-5	32	Very coarse	} Gravel
-4	16	Coarse	
-3	8	Medium	
-2	4	Fine	
-1	2	Very fine	
0	1	Very coarse	} Sand
1	500 microns	Coarse	
2	250	Medium	
3	125	Fine	
4	63	Very fine	
5	31	Very coarse	} Silt
6	16	Coarse	
7	8	Medium	
8	4	Fine	
9	2	Very fine	
		Clay	

4.6 Estuarine Sediments

The bottom sediments from Karli River estuary were collected during Post monsoon (Nov.2016).The estuarine bottom sediment samples collected during this season (Nov. 2016) were subjected to textural analysis. One portion of the bulk sample was subjected to sieve analysis. The sieve analysis data (weight percent and cumulative percent) was used for grain size parameters mean size, standard deviation, skewness and kurtosis which are presented in Table 3 and 4 are presented

to show the percentage abundance of these textural parameters. Further it is noted that majority of Karli River estuary sediments show dominance of medium sand (85%-98%). The sorting values indicate that the sediments are mainly well sorted to moderately well sort at Karli River. The Karli River. Estuarine sediments during postmonsoon are positively skewed and nearly symmetrical in nature observed in the table 5 and 6. The kurtosis values show that the Gad R. estuarine sediments during postmonsoon are overall Leptokurtic can be clearly

observed in the table 3.4(B). The depth vs turbidity graph is plotted in Fig 2 from the data taken in the field. This graph shows that the turbidity is almost constant at all 25 stations where samples were collected. It is clear from the data, the sediment texture during postmonsoon is dominated by the sand fraction ranging from 88 – 98 %, the average being 95%. The dominating sand fraction in the sediments of this estuary can be attributed to high sediment input from inland by the erosion and surface runoff through the catchment. This contribution from the inland has given rise to

formation of several islands in the estuary. The high concentration of sand can also be attributed to the flood tidal influence. This is evident by the recent deposits of bars at the river mouths and formation of lagoon.

4.7 Downstream Variations

The downstream variations of mean size and standard deviation with bivariate plots of mean size vs standard deviation and skewness has been presented in figure (A-D).

Method of Moments.

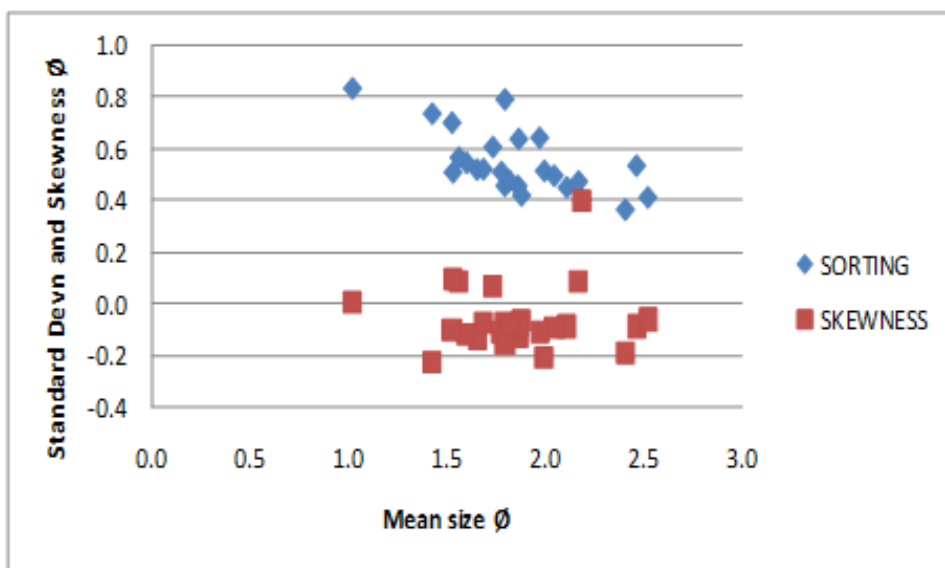


Fig. A

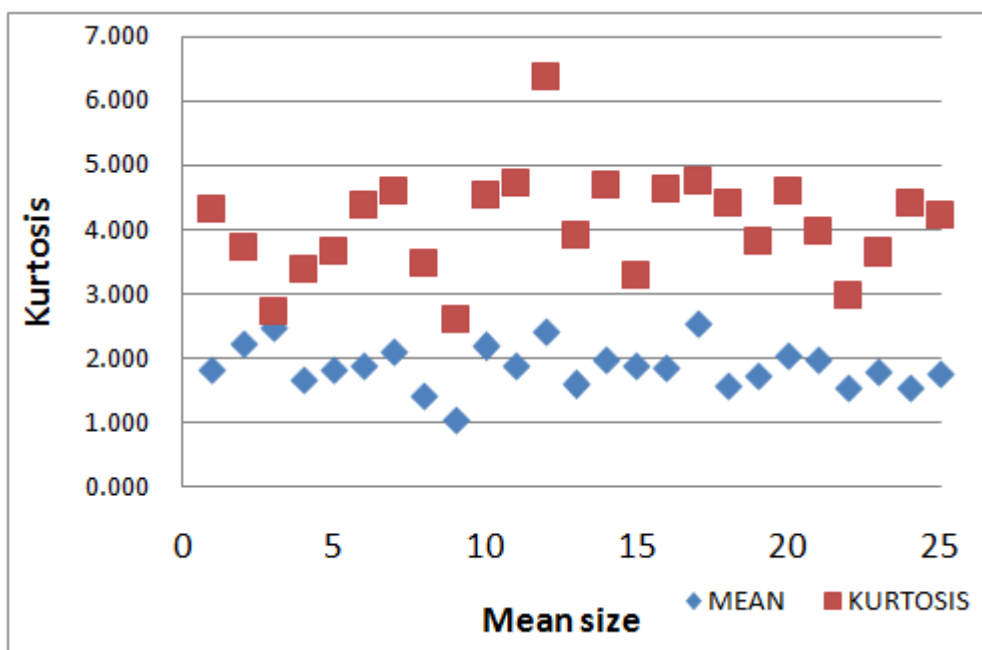


Fig. B

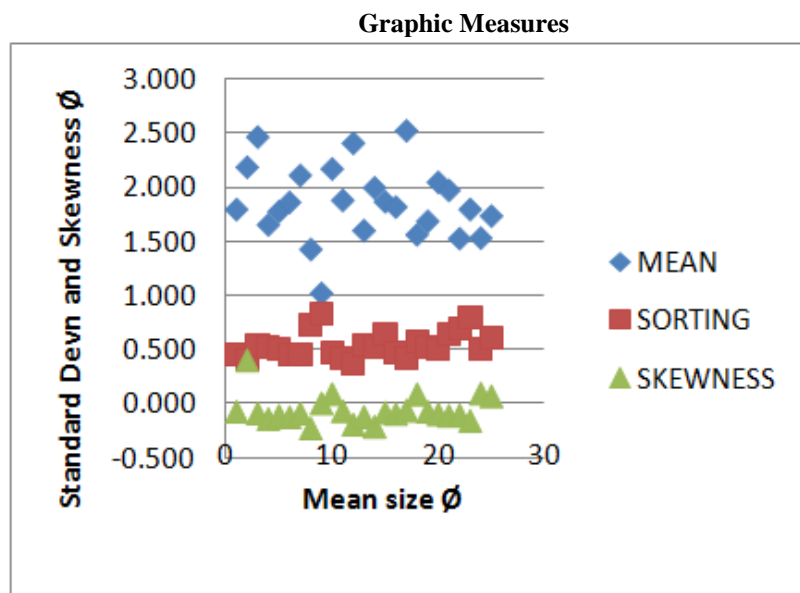


Fig. C

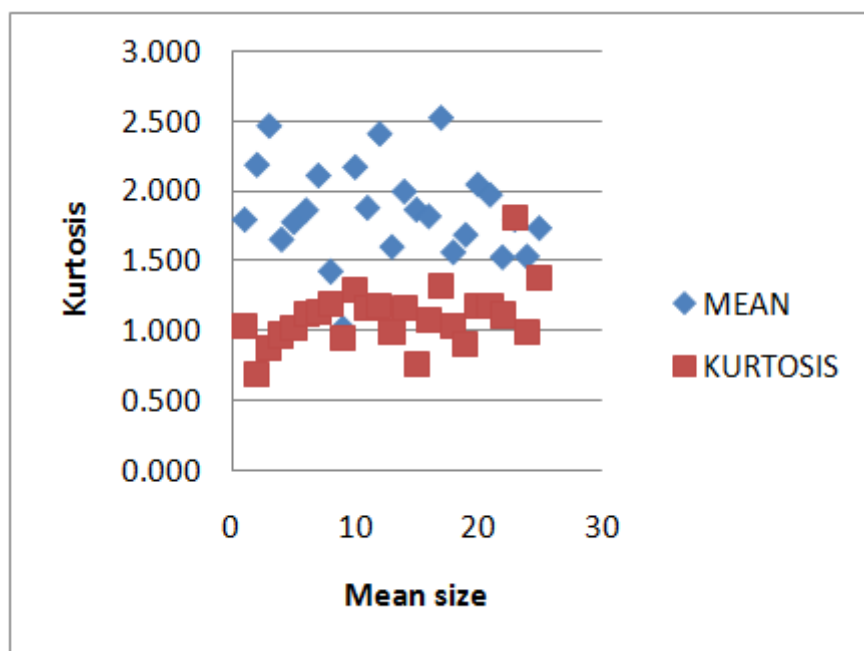


Fig. D

Fig 3.2(A-D).Bivariant plots of grain size parameters of sediment samples collected at estuary during postmonsoon seasons.

In general, Karli River. estuarine sediment mean size during the postmonsoon season show seaward (downstream) fining trend. Similarly, the sorting also increases in the downstream direction. The bivariant plots of mean size vs. standard deviation and skewness for Karli River. estuary sediments shows that the postmonsoon sediments scatter separately. The postmonsoon sediments are medium grained (1.5-2 ϕ), well sorted and negative to near symmetrical in nature.

4.8 Sediment Movement at the estuaries

The sediment transport paths deduced for Karli River estuaries have been presented in the above said Table and figure. During postmonsoon (Nov. 2016), the Karli River, estuary shows a strong seaward transport trend representing a low energy regime.

4.9 Bivariant Plots:

Bivariant plots between certain parameters are also helpful to interpret the energy conditions, medium of transportation, mode of deposition etc.

Passega (1957), Visher (1969), Folk and Ward (1957) and others described that these trends and interrelationship exhibited in the bivariate plots might indicate the mode of deposition and in turn aid in identifying the environments. However, Mason and Folk (1958), Friedman (1961) claimed to establish the differentiation between aeolian, beach and river sediments based on these bivariate plots. An attempt has been made here to utilize these approaches and prepare the bivariate plots for the Karli river estuary sediments. The interrelationship between mean grain size vs. standard deviation and skewness for all the seasons are shown in the figure. This shows that the degree of sorting increases with increase in the mean size. The plot between the mean size and kurtosis shows that the spread of sediments increases with increase in the mean size. The bivariate plot of simple sorting measure vs simple skewness measure is plotted following Friedman (1967, 1979) to understand the processes under which the sediment has been deposited. The nature of the sediments is dominantly bimodal of which the dominant constituent is medium sand.

4.10 CM Patterns

Passega (1957) interpreted the distinct patterns of CM plots in terms of different modes of transportation by plotting coarsest first percentile grain size (C) and the median size (M) of sediment samples on a double log paper. The CM pattern of the sedimentary environment help in analyzing transportation mechanism, depositional environment with respect to size, range and energy level of transportation it also determines process and segregates characteristic agents that are responsible for the formation of clastic deposits. In the present study an attempt has been made to identify the modes of deposition of the sediments of the Karli river estuary by CM patterns. Visher (1969) explained the log normal sub populations within the total grain size distribution curve as representing suspension, saltation and surface creep or rolling modes of transportational mechanisms. The relation between C and M is the effect of sorting by bottom turbulence. The good correlation between C, determined by only one percent by weight of the sample, and M, which represents grain size as a whole, shows the precision of the control of sedimentation by bottom turbulence. The results have been plotted in CM diagram. Passega (1964, 1977); Kumar and Singh (1978) have used the grain size parameters and the plots of CM patterns to distinguish between the sediments of different environments. The sediments of the study area do not fall in the 'S' field as given by Passega and Byramjee (1969) which is the area for tractive currents of beach sediments. However, the sediments of the study area fall in the fields I, II and

III which suggest that: Point no I in the Fig represents deposition from rolling. Points of zone II represent deposition from rolling and suspension. The remaining one sample at point III represents the deposition from graded suspension with high turbulence. No samples show graded suspension with low turbulence. The CM plot also shows that most of the sediment samples fall in the intermediate position between P and R. Segment PQ indicates the coarse grains transported by rolling, while QR parallel to line C=M represents the main channel deposits. RS parallel to the M axis indicates the uniform suspension. This PR segment exhibits that the Karli estuary sediments underwent rolling which are the prime factors for transportation (Table 4).

4.11 Linear Discriminant Function (LDF) Analysis of the Sediments.

The multivariate linear discriminate function analysis (Sahu, 1964) was used for the sediments of the study area for all the seasons. It is observed from the table and figure., that the majority of the sediment samples (91%) of the study area during the post monsoon seasons fall in beach environment and about 9% of the sediment samples represent Aeolian processes (backshore or fore dune samples). Further discrimination among beach and shallow marine processes (Y2), shows that the sediments of the study area are predominantly represent shallow marine environment (45%), where as 48% represent beach processes, remaining 3% shows Aeolian deposition. This indicates that the sediments are circulated seaward (monsoon) and landward (fair-weather) otherwise, It is also possible that the sediments in the present-day beaches must have been deposited in a shallow marine environment and later the marine regression must have led to the development of the present-day shorelines (Angusamy and Rajamanickam, 2007). Lastly, the discrimination between marine and fluvial processes (Y3) shows that majority of the sediments represent marine processes (100%). Tables 4, 5 and 6.

Sample	METHOD OF MOMENTS				GRAPHIC MEASURES			
	Mean	Sorting	Skewness	Kurtosis	Mean	Sorting	Skewness	Kurtosis
1	1.825	0.479	0.276	4.294	1.796	0.456	-0.072	1.034
2	2.218	0.450	0.747	3.731	2.186	0.403	0.401	0.682
3	2.484	0.527	0.191	2.714	2.464	0.534	-0.088	0.874
4	1.656	0.521	-0.069	3.366	1.655	0.519	-0.140	0.963
5	1.823	0.533	0.265	3.648	1.778	0.509	-0.111	1.012
6	1.875	0.480	-0.153	4.357	1.862	0.455	-0.123	1.116
7	2.096	0.481	0.091	4.577	2.110	0.450	-0.088	1.127
8	1.415	0.731	-0.559	3.477	1.428	0.735	-0.227	1.183
9	1.052	0.786	0.329	2.606	1.023	0.833	0.005	0.946
10	2.175	0.493	0.513	4.530	2.170	0.473	0.090	1.288
11	1.894	0.451	0.145	4.704	1.880	0.419	-0.068	1.156
12	2.401	0.430	-0.519	6.361	2.407	0.364	-0.191	1.168
13	1.583	0.577	-0.132	3.908	1.602	0.545	-0.121	0.984
14	1.978	0.557	-0.604	4.690	1.996	0.514	-0.210	1.160
15	1.878	0.673	0.163	3.270	1.866	0.637	-0.080	0.756
16	1.849	0.532	0.143	4.632	1.819	0.475	-0.094	1.073
17	2.519	0.442	-0.159	4.733	2.521	0.411	-0.062	1.318
18	1.561	0.607	0.466	4.412	1.563	0.565	0.089	1.026
19	1.715	0.566	0.272	3.817	1.687	0.520	-0.072	0.896
20	2.034	0.539	-0.126	4.587	2.046	0.495	-0.095	1.169
21	1.976	0.659	-0.238	3.973	1.972	0.642	-0.109	1.170
22	1.528	0.702	0.034	2.982	1.528	0.700	-0.103	1.107
23	1.773	0.745	-0.488	3.639	1.796	0.791	-0.156	1.806
24	1.531	0.541	0.411	4.399	1.533	0.508	0.095	0.985
25	1.742	0.655	0.453	4.200	1.735	0.606	0.069	1.372

Table 7 Grain size parameters of Karli river estuary sediment samples:

Table 8 Grain size distribution of estuarine sediments based on textural classes

Sample no.	% V Coarse:	% Coarse:	% Medium:	% Fine Sand:	% V Fine Sand:
1	0.00%	2.20%	61.70%	34.70%	1.40%
2	0.00%	0.10%	46.10%	51.30%	2.50%
3	0.00%	0.20%	26.80%	60.30%	12.70%
4	0.00%	8.00%	66.60%	24.40%	1.10%
5	0.00%	4.30%	57.80%	35.70%	2.20%
6	0.00%	2.90%	55.20%	41.00%	1.00%
7	0.00%	2.50%	34.00%	60.40%	3.10%
8	6.10%	15.70%	57.00%	20.30%	0.90%
9	11.70%	34.40%	40.00%	12.40%	1.60%
10	0.00%	0.60%	31.40%	62.90%	5.20%
11	0.00%	1.70%	57.80%	39.20%	1.40%
12	0.00%	0.80%	9.90%	84.00%	5.30%
13	0.00%	11.50%	65.70%	21.60%	1.20%
14	0.50%	3.90%	38.20%	55.20%	2.10%
15	0.00%	5.00%	48.00%	42.60%	4.30%
16	0.20%	3.60%	57.20%	36.30%	2.60%

17	0.00%	0.30%	7.40%	79.30%	12.90%
18	0.00%	12.00%	66.20%	20.10%	1.80%
19	0.50%	3.30%	75.50%	19.40%	1.30%
20	0.00%	2.90%	39.90%	53.70%	3.50%
21	0.80%	5.20%	40.40%	48.50%	5.10%
22	0.00%	18.80%	56.00%	21.10%	4.10%
23	1.70%	14.30%	55.30%	26.10%	2.60%
24	0.20%	10.50%	71.60%	16.60%	1.20%
25	0.00%	10.90%	57.80%	26.50%	4.80%

Table 9 Grain Size Analysis

sample no.	Mean:	Sorting:	Skewness:	Kurtosis:
1	Medium Sand	Well Sorted	Symmetrical	Mesokurtic
2	Fine Sand	Well Sorted	Very Fine Skewed	Platykurtic
3	Fine Sand	Moderately Well Sorted	Symmetrical	Platykurtic
4	Medium Sand	Moderately Well Sorted	Coarse Skewed	Mesokurtic
5	Medium Sand	Moderately Well Sorted	Coarse Skewed	Mesokurtic
6	Medium Sand	Well Sorted	Coarse Skewed	Leptokurtic
7	Fine Sand	Well Sorted	Symmetrical	Leptokurtic
8	Medium Sand	Moderately Sorted	Coarse Skewed	Leptokurtic
9	Medium Sand	Moderately Sorted	Symmetrical	Mesokurtic
10	Fine Sand	Well Sorted	Symmetrical	Leptokurtic
11	Medium Sand	Well Sorted	Symmetrical	Leptokurtic
12	Fine Sand	Well Sorted	Coarse Skewed	Leptokurtic
13	Medium Sand	Moderately Well Sorted	Coarse Skewed	Mesokurtic
14	Medium Sand	Moderately Well Sorted	Coarse Skewed	Leptokurtic
15	Medium Sand	Moderately Well Sorted	Symmetrical	Platykurtic
16	Medium Sand	Well Sorted	Symmetrical	Mesokurtic
17	Fine Sand	Well Sorted	Symmetrical	Leptokurtic
18	Medium Sand	Moderately Well Sorted	Symmetrical	Mesokurtic
19	Medium Sand	Moderately Well Sorted	Symmetrical	Platykurtic
20	Fine Sand	Well Sorted	Symmetrical	Leptokurtic
21	Medium Sand	Moderately Well Sorted	Coarse Skewed	Leptokurtic
22	Medium Sand	Moderately Sorted	Coarse Skewed	Mesokurtic
23	Medium Sand	Moderately Sorted	Coarse Skewed	Very Leptokurtic
24	Medium Sand	Moderately Well Sorted	Symmetrical	Mesokurtic
25	Medium Sand	Moderately Well Sorted	Symmetrical	Leptokurtic

Fig 3. Sand-Silt-Clay Diagram



Table 4 CM pattern values (phi values) obtained by plotting cumulative weight % against particle size on a probability graph sheets.

Sample no	Phi 1	Phi 50	Phi 1(μ)	Phi 50(μ)
1	0.85	1.85	850	1850
2	1.42	2.4	1420	2400
3	1.43	2.58	1430	2580
4	0.4	1.75	400	1750
5	0.62	1.88	620	1880
6	0.6	1.95	600	1950
7	0.8	2.1	800	2100
8	-1	1.5	-1000	1500
9	-1.8	1.1	-1800	1100
10	1.3	2.15	1300	2150
11	0.8	1.9	800	1900
12	1.2	2.5	1200	2500
13	0.2	1.65	200	1650
14	0.2	2.4	200	2400
15	0.23	1.93	230	1930
16	0.5	1.85	500	1850
17	1.25	2.58	1250	2580
18	0.18	1.6	180	1600
19	0.45	1.8	450	1800
20	0.55	2.1	550	2100
21	0.1	2.05	100	2050
22	0.21	1.55	210	1550
23	0.28	1.85	280	1850
24	0.22	1.5	220	1500
25	0.5	1.75	500	1750

Table 5 Linear Discriminant Function (LDF) analysis of the beach sediments.

Y1	Y2	Y3
1.854316	79.24216	-5.76978
1.851631	99.78459	-4.1146
0.025212	74.76576	-3.30377
1.060661	75.67839	-3.16623
-0.70382	77.92544	-2.99268
-1.38355	66.07646	-2.73997
-5.9072	64.79548	-2.73265
-2.63654	68.44297	-2.5966
-1.64348	77.61657	-2.45666
-1.64535	60.88383	-2.23928
-3.0922	74.11433	-1.71814
-1.29993	60.6423	-1.51109
-2.07735	59.46608	-1.49383
-4.83279	71.85286	-1.31814
-2.00324	61.60592	-1.17538
-1.61926	58.89701	-1.15953
-2.55878	68.04546	-1.04214
-2.1174	61.49161	-0.9504
-2.2671	59.61374	-0.90842
-3.09021	65.57713	-0.68451
-2.09803	66.23457	-0.65857
-2.14608	61.20323	-0.62877
-2.32081	61.12082	-0.61371
-4.13828	73.85187	-0.39654
-4.06565	64.5272	0.516724

Table 6

Total samples	Aeolian:Beach (Y1)		Beach: Shallow Marine (Y2)		Shallow Marine:Fluvial (Y3)	
	Aeolian (<-2.7411)	Beach (>-2.7411)	Beach (<65.3650)	Shallow Marine (>65.3650)	Marine (<-7.4190)	Shallow Fluvial (>-7.4190)
25	6	19	11	14	25	-

Table 7 GPS reading of the sampling location, depth of sampling at Karli River. Estuary

Sample numbers	latitude	Longitude	depth	elevation(ft)	Turbidity
M1	15.96613	73.50436	1.5	9	1.5
M2	15.97155	73.50407	1.5	11	1.5
M3	15.97391	73.50417	0.5	36	0.5
M4	15.97751	73.50279	2	16	1.75
M5	15.983	73.49855	2	16	1.8
M6	15.98238	73.49726	2.8	14	2.8
M7	15.98618	73.49515	4	20	2
M8	15.9907	73.49394	3	11	1.5
M9	15.99163	73.49309	3	14	2
M10	15.99647	73.49226	1.5	13	1.5
M11	15.99774	73.49544	2.3	18	1.5
M12	16.00102	73.49284	2.3	12	1.5
M13	16.00491	73.49813	3.5		1.5
M14	16.00788	73.4957	2	16	1.4
M15	16.00958	73.50007	1.8	17	1.8
M16	16.00794	73.50365	1.5		1
M17	16.0109	73.5059	0.9	17	0.9
M18	16.01102	73.51154	3.5		1.3
M19	16.01361	73.51118	1.2	17	1.2
M20	16.0164	73.5158	3	16	1.2
M21	16.01551	73.52096	3.3	18	1
M22	16.01676	73.52614	3.5	14	1
M23	16.01721	73.5301	3.3	21	1.2
M24	16.01692	73.53428	4	16	0.8
M25	16.01675	73.5385	3.3	20	1.2

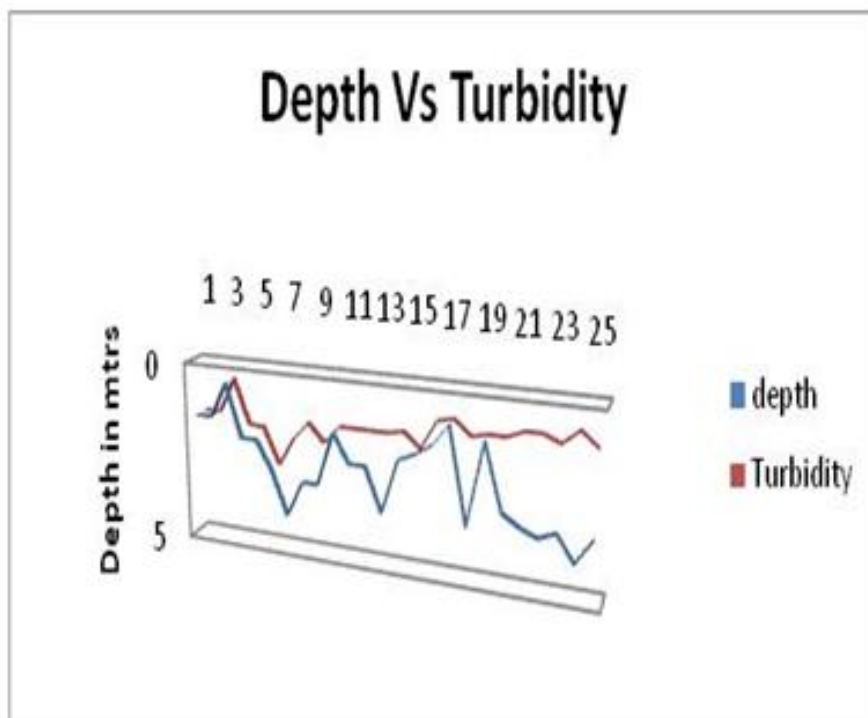
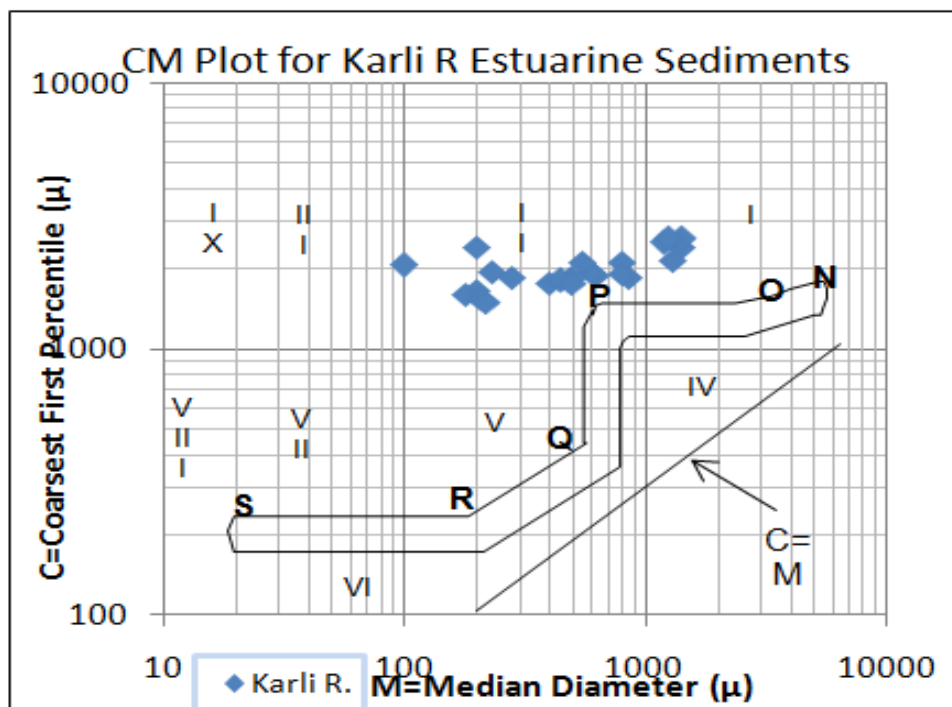


Fig 4 Depth vs Turbidity plot using field data

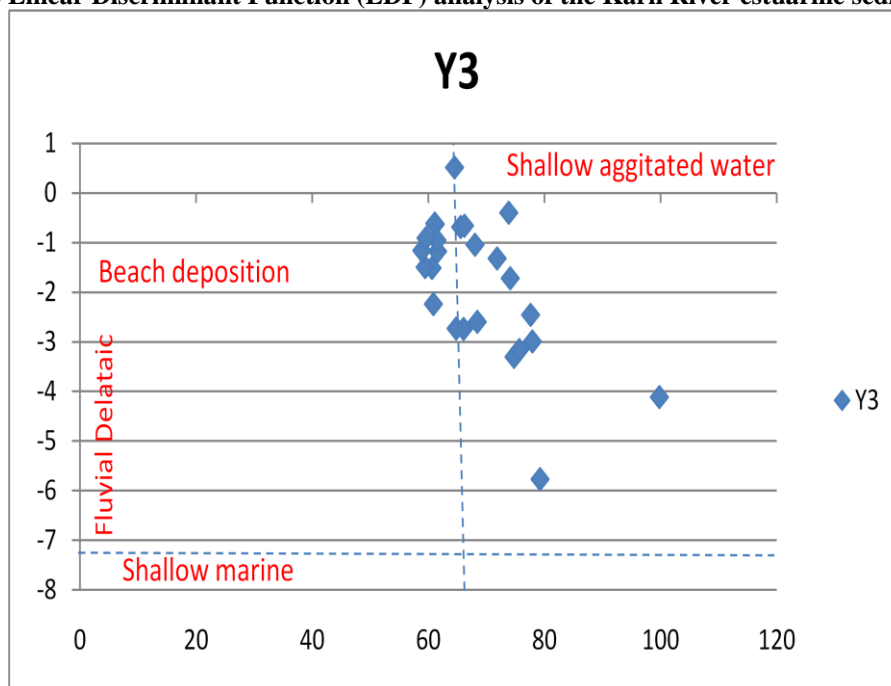
Fig 5 CM pattern of the Sediments of Karli River Estuary



The CM pattern of the sedimentary environment help in analyzing transportation mechanism, depositional environment with respect to size, range and energy level of transportation and also determines process and segregates characteristic agents that are responsible for the formation of

clastic deposits. The CM plot at the present study shows that most of the sediment samples fall in the intermediate position between P and R. This PR segment exhibits that the Karli estuary sediments underwent rolling which are the prime factors for transportation.

Fig 6 Linear Discriminant Function (LDF) analysis of the Karli River estuarine sediments



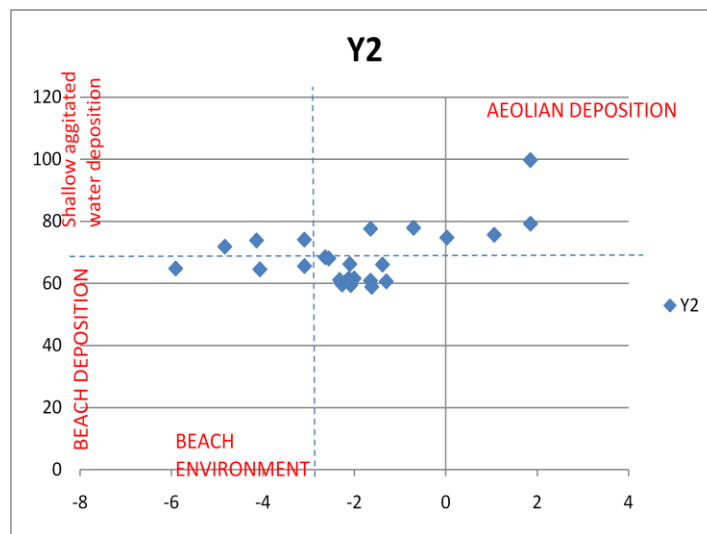
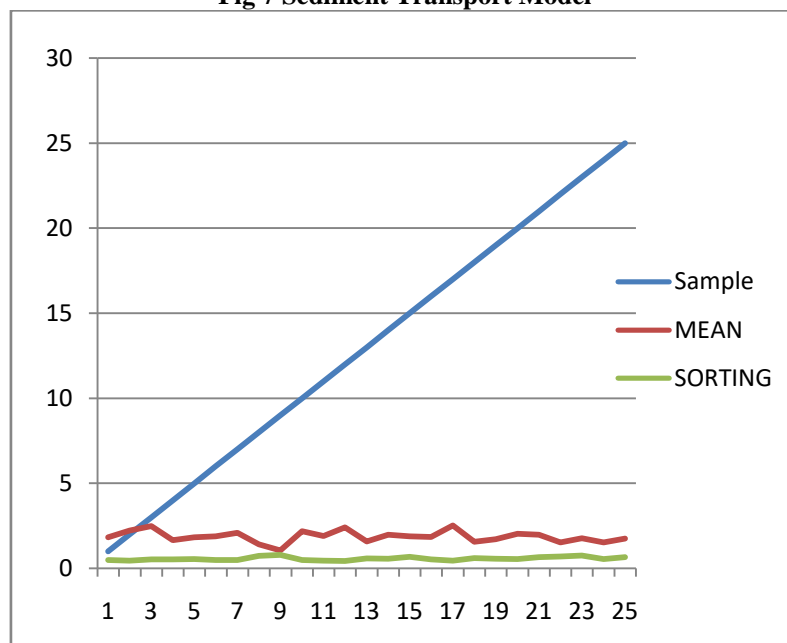


Fig 7 Sediment Transport Model



V. CONCLUSION

The major part of Karli River estuary sediments show dominance of medium sand (85%-98%), the average being 95%. The postmonsoon sediments are medium grained (1.5-2 ϕ), well sorted and positively skewed and near symmetrical in nature. The kurtosis values show that the Karli River estuarine sediments during postmonsoon are overall Leptokurtic. The sediment transport paths deduced for Karli River estuaries has been presented in table 3.3 and figure 3.5. During postmonsoon (Nov. 2016), the Karli River estuary shows a strong seaward transport trend representing a low energy regime. The bivariate plots between mean size Vs. standard deviation and skewness for all the seasons is presented. This shows that the degree of sorting increases with

increase in the mean size. The CM plot at the present study shows that the Karli River estuary sediments underwent rolling which are the prime factors for transportation. The multivariate linear discriminant function analysis shows that the majority of the sediment samples (91%) of the study area during the post monsoon seasons fall in beach environment and about 9% of the sediment samples represent Aeolian processes (backshore or fore dune samples). The quantitative morphometric analysis using SRTM data and GIS techniques is a simple economical and time saving methodology to study the river basin with an output of good quality and high degree of accuracy. Karli river sub basin geology is reasonably homogeneous without structural disturbances which is elongated in shape and hence will have a flatter peak of flow for

longer duration lower efficiency in discharge of run-off.

Recommendation

Taking into consideration of the changing climatic conditions the data base on all the beaches regarding morphology, texture and dynamic processes are quite significant all along the Maharashtra coast, which provide ample opportunity to study the paleo-climate, sea level changes and coastal evolution on local and regional scale. All the above outputs clearly lead to the conclusion that the Karli river sub basin has the potential to perform its drainage function more effectively. Increasing the storage capacity of the water bodies, rehabilitation and restoring channels to standards will enhance the sub basins water holding capacity which will be of immense use to meet the urban water demands of the Malwan area apart from meeting the agriculture, domestic and industrial demands.

REFERENCES

- [1] Angusamy N., Rajamanickam G.V., 2007, Coastal processes of central Tamil Nadu, India: clues from grain size studies, *Oceanologia*, 49 (1), 41– 52
- [2] Blott, S. J., and Pye, K. 2001. GRADISTAT: A grain size distribution and statistics package for the analysis of unconsolidated sediments. *Earth Surfaces Processes and Landforms*, 26: 1237–1248.
- [3] Dalrymple, R. W., Zaitlin, B. A., and Boyd, R., 1992. Estuarine facies models; conceptual basis and stratigraphic implications. *Journal of Sedimentary Petrology*. 62, pp 1130-1146.
- [4] Defra 2002, http://www.estuary-guide.net/guide/chapter3_estuary_setting.asp
- [5] Folk RL. 1954. The distinction between grain size and mineral composition in sedimentary-rock nomenclature. *Journal of Geology* 62: 344–359.
- [6] Folk RL, Ward WC. 1957. Brazos River bar: a study in the significance of grain size parameters. *Journal of Sedimentary Petrology* 27: 3–26.
- [7] Friedman, G.M. (1961): Distinction between Dune, Beach and River sands from their textural characteristics. *Jour. Sed. Pet.*, V-31, p 514-529.
- [8] Friedman, G.M. (1967): “Dynamic processes and statistical parameters compared for size frequency distribution of Beach and River sands,” *Jour. Sed. Pet.*, vol. 37, p. 327-354.
- [9] Friedman, G. M. 1979a. 'Address of the Retiring President of the International Association of Sedimentologists: differences in size distributions of populations of particles among sands of various origins', *Sedimentology*, 26, pp. 3-32.
- [10] Friedman, G. M. 1979b. 'Differences in size distributions of populations of particles among sands of various origins: addendum to IAS Presidential Address', *Sedimentology*, 26, pp. 859- 862.
- [11] Hanamgond, 2012, *Estuarine Dynamics of Kalavali, Kolamb and Karli Rivers With Special Reference to their Impact on the Malvan Coast, Sindhudurg District, Maharashtra UGC Major Research Project (F. 33-42/2007 (SR) 28/2/08)*, 268p.
- [12] Kumar, S. and Singh, I.B. (1978). *Sedimentological study of Gomati River sediments, Uttar Pradesh, India. Example of a river in Alluvial Plain. Senckenbergiana marit*, v.10, pp.145-211.
- [13] Krumbein WC, Pettijohn FJ. 1938. *Manual of Sedimentary Petrography*. Appleton-Century-Crofts: New York.
- [14] Mason, C.C. and Folk R.L. (1958): Differentiation of beach, dune and aeolian flat environment by size analysis, *Mustang Island, Texas, Jour. Sed. Pet* vol. 28, p 211-226.
- [15] McLaren, P., 1981. An interpretation of trends in grain size measures. *Jour. Sed. Petrol.*, v. 51, pp. 611-624.
- [16] McLaren, P. and Bowles, D., 1985. The effects of sediment transport on grain size distributions. *Jour. Sed. Petrol.*, v. 55, pp. 457-470.
- [17] Passega R., 1957. Texture as characteristic of clastics deposition: *Am. Soc. Asoc. Petrol. Geol. Bull. Tulsa, Okland*, 41, 1952-1984.
- [18] Passega, R. (1964): Grain size representation by CM patterns as geological tool. *Jour. Sed. Pet.*, vol. 34, p. 830-847.
- [19] Passega, R. & Byramjee, R., 1969. Grain-size image of clastic deposits. *Sedimentology* 13, 233–252.
- [20] Sahu BK. 1964. Depositional mechanism from size analysis of clastic sediments. *Tulsa, USA. J Sed Petrol* 34: 73-83.
- [21] Shirodkar S.R* and V.N. Nayak. Distribution and Seasonal Abundance of Macro Benthos of Gangavali Estuary, Uttar Kannada, West Coast of India. *Journal of Ecobiotechnology* 2/5: 80-84, 2010; ISSN 2077-0464;
- [22] Sugirtha P. Kumar and M.S.Sheela Studies on the Sediment Characteristics of

- Manakudy Estuary, South west coast of India; *International Research Journal of Environment Science*; Vol. 2(11), 78-83, November (2013);
- [23] Udden, J.A. (1914): Mechanical composition of clastic sediments. *Geol. Soc. Am. Bull.* Vol. 25 p. 655-744.
- [24] Visher, G.S. (1969): Grain size distribution and depositional process, *Jour, Geol* V-39, P1074-1106.
- [25] Wentworth, CK (1922): A scale of computing mechanical composition types in sediments *Geol. Soc. Am. Bull.* vol. 40, p 771.

International Journal of Engineering Research and Applications (IJERA) is **UGC approved** Journal with Sl. No. 4525, Journal no. 47088. Indexed in Cross Ref, Index Copernicus (ICV 80.82), NASA, Ads, Researcher Id Thomson Reuters, DOAJ.

Shivani hulaji. "Grain Size Analysis of Karli River Estuarine Sediments Sindhudurg, Maharashtra, India." *International Journal of Engineering Research and Applications (IJERA)* , vol. 7, no. 10, 2017, pp. 41–62.